INTERNATIONAL JOURNAL OF AGRICULTURE & BIOLOGY
ISSN Print: 1560–8530; ISSN Online: 1814–9596
16–0809/2017/19–4–865–872
DOI: 10.17957/IJAB/15.0376
http://www.fspublishers.org

Full Length Article

Characterization of LhSorPR5, a Thaumatin-like Protein from the Oriental Hybrid Lily Sorbonne

Le Wang[1,2], Lanjun Li[3], Yubao Zhang[1], Zhihong Guo[1], Yajun Wang[1], Guo Yang[1], Li Wang[4], Ruoyu Wang[1] and Zhongkui Xie[1*]

[1]*Gaolan Station of the Agricultural and Ecological Experiment, Northwest Institute of Eco-Environment and Resources, Chinese Academy of Sciences, Lanzhou 730000, China*
[2]*University of Chinese Academy of Sciences, Beijing 100049, China*
[3]*College of Life Sciences of Northwest Normal University, Lanzhou, China*
[4]*The Forest Tree Seedling Station of the Alxa League, Alxa League 750300, China*
[*]For corresponding: wxhcas@lzb.ac.cn; zhongkuixiecas@yahoo.com

Abstract

Pathogenesis-related (PR) proteins are widely involved in plant defense against both biotic and abiotic stresses. Among the 17 PRs classified, the PR5 family has been found in numerous plant species. In this study, a PR5 protein from the oriental hybrid lily cultivar Sorbonne (designated LhSorPR5) was characterized. The isolated full-length cDNA was 1391 bp, consisting of a 5′ untranslated region (UTR) of 137 bp, a predicted open reading frame (ORF) of 939 bp, and a 3′ UTR of 315 bp. The predicted ORF encoded a protein of 312 amino acids with a 22-amino-acid signal peptide located at the N-terminus. The mature LhSorPR5 (devoid of a signal peptide) had a theoretical isoelectric point of 4.5 and a calculated molecular weight of 30.49 kDa. The deduced LhSorPR5 shared high similarity to PR5 orthologues originating from other plants. Using homology modeling, a three-dimensional model of LhSorPR5 was built, and an acidic cleft which formed by five conserved REDDD residues was found in the model constructed. *LhSorPR5* transcript levels in response to different stress treatments were quantified using qPCR and *LhSorPR5* expression was induced by salt, polyethylene glycol (PEG), *Botrytis elliptica* infection, and phytohormones (methyl jasmonate, sodium salicylate, ethephon and abscisic acid) treatments. The His_6-tagged LhSorPR5 recombinant protein was expressed in *Escherichia coli* and successfully purified. The *LhSorPR5* characterized in this study is the first *PR5* family gene to be isolated from *Lilium*, and it could potentially be used as an aid in future studies on lily disease resistance. © 2017 Friends Science Publishers

Keywords: Disease resistance; Expression analysis; Homology modeling; Lily; Pathogenesis-related protein

Introduction

Being sessile, plants are vulnerable to biotic and abiotic stress. To combat this, plants have evolved a highly complex and multilayered immune system to detect and counteract potential pathogenic organisms in the environment. Generally, the innate immunity of plants could be divided into two distinct branches: pathogen-associated molecular pattern (PAMP) triggered immunity (PTI) and effector-triggered immunity (ETI) (Jones and Dangl, 2006). The activation of ETI is often accompanied by hypersensitive responses, accumulation of antimicrobial chemicals, and induced expressions of pathogenesis-related (PR) proteins (Glazebrook, 2005). Based on amino acid sequences, protein structures, and antimicrobial mechanisms, PR proteins have been classified into 17 families (van Loon *et al*., 2006). Although PR proteins are closely related to pathological processes, it is worth noting that PR family proteins do not all exhibit enzymatic activity that is directly related to antimicrobial functions. Proteins in the PR5 family exhibit glucanase activity that is related to antifungal activity (Anzlovar and Dermastia, 2003). PR5 proteins are also referred to as thaumatin-like proteins (TLP) due to their high similarity to thaumatin, a sweet-tasting protein originating from *Thaumatococcus danielli* (Edens *et al*., 1982). Originally, TLPs were first identified in virus infected tobacco (Cornelissen *et al*., 1986). Later studies revealed that TLP was a group of proteins widely involved in plant defense mechanisms. Not only do they inhibit fungal infections and growth, they also function as a response mechanism of plants to osmotic stress (Singh *et al*., 1987). In *Ocimum basilicum*, *ObTLP1* expression was significantly induced by dehydration and salt stress (Misra *et al*., 2016), and overexpression of *ObTLP1* conferred enhanced tolerance to mannitol and salt stress in *Arabidopsis*. Similarly, *AsPR5* from garlic (*Allium sativum L.*) was also upregulated by dehydration, high salinity, and phytohormones in different types (Rout *et al*., 2016),

To cite this paper: Wang, L., L. Li, Y. Zhang, Z. Guo, Y. Wang, G. Yang, L. Wang, R. Wang and Z. Xie, 2017. Characterization of LhSorPR5, a thaumatin-like protein from the oriental hybrid lily Sorbonne. *Int. J. Agric. Biol.,* 19: 865–872

suggesting diverse roles PR5 may play in plant defense. Typical TLPs are small (from 20 to 26 kDa), composed of 16 conserved cysteine residues that form eight disulfide bridge pairs. At the present time, the crystal structure of some TLPs have been resolved (Ghosh and Chakrabarti, 2008), and an acidic cleft that catalyzes the hydrolysis of β-1,3-glucan has been found in presence of certain TLPs. Given that β-glucan is the structural component of fungi cell walls, glucanase activity that enables the degradation of cell wall is highly significant to the antifungal properties of TLPs.

Lilies are perennial bulbous flowers that emit strong fragrance. Accordingly, they are popular throughout the world. Nearly three million lily bulbs are commercially produced each year, for which over 90% are used for cut flower production (Buschman, 2005). Nevertheless, lily production, from bulbs to cut flowers, is severely affected by different types of pathogens. For instance, lily bulbs could be infected by the fungal pathogen *Fusarium oxysporum* f. sp. *lilii* (Curir *et al*., 2000), which causes bulb base, bud, and scale rot. During plant growth, moreover, *Botrytis cinerea* and *B. elliptica* infections (Liu *et al*., 2008) could lead to the destructive fire blight disease, which severely affects cut flower production. Furthermore, parasite infection and viral multiplication, such as those caused by the lily mottle virus (LMoV) (Zhang *et al*., 2015a), the cucumber mosaic virus (CMV) (Niimi *et al*., 2003), and the lily symptomless virus (LSV) (Zhang *et al*., 2015b), result in leaf mottle and contortion as well as the stunted growth of lilies. To prevent such damage from pathogenic organisms, greater information on genes (including PR proteins) that govern plant immunity response would be of great importance.

In this study, we characterized a TLP from the oriental hybrid lily cultivar Sorbonne (designated LhSorPR5). Sequence alignments revealed that LhSorPR5 shares a high level of identity and similarity to PR5s originating from other plants. We built a three-dimensional LhSorPR5 model by which we detected an acidic cleft. Further gene expression analysis showed that *LhSorPR5* expressions were responsive to phytohormone and stress treatments.

Materials and Methods

Plant Material and Growth Conditions

The oriental hybrid lily cultivar Sorbonne was selected for this study. We planted one bulb from 10 to 12 cm in diameter in each pot (25 cm in diameter) containing peat moss as a growing substrate. We then moved the pots into a growth chamber until use and kept the bulbs under optimum growth conditions (16 h light/8 h dark; 22°C). We stored all bulbs at 4°C for over 2 months to end the lily dormant state before the experiment started.

Total RNA Isolation and First-strand cDNA Synthesis

We conducted total RNA isolation using the RNAprep Pure Kit for plants (TIANGEN Corporation, Beijing, China) following the manufacturer's instructions. We evaluated the quality and quantity of the RNA extracted applying 260/280 and 260/230 absorbance ratios using a Nanodrop 2000c spectrophotometer (Thermo Fisher Scientific, USA). Additionally, we reversely transcribed 5 μg of total RNA into cDNA using the PrimeScript II First Strand cDNA Synthesis Kit (Takara Biotechnology, Dalian, China). For cDNA synthesis of rapid amplification of cDNA ends (RACE) cloning, we used 1 μg of total RNA for first-strand cDNA synthesis.

Full-length *LhSorPR5* Cloning

To obtain the partial coding sequence of *LhSorPR5*, we designed a pair of degenerate primers (PR5-deg-F and PR5-deg-R; Table 1) based on conserved regions of PR5 proteins. We designed gene-specific primers (GSP) for 5′RACE (Table 1) (PR5-5RACE-GSP-1 and PR5-5RACE-GSP-2) and 3′RACE (PR5-3RACE-GSP-1 and PR5-3RACE-GSP-2) based on the partial coding sequence obtained to conduct RACE cloning. All polymerase chain reaction (PCR) products were gel purified and ligated into pMD18T vectors for sequencing. We obtained the full-length sequence of *LhSorPR5* by assembling the 5′RACE sequence, the partial coding sequence, and the 3′RACE sequence.

In silico Analysis of LhSorPR5

We predicted the open reading frame (ORF) of the full-length *LhSorPR5* sequence using the ORF finder. We confirmed the homology of the LhSorPR5 protein sequence to other proteins by querying the National Center for Biotechnology Information (NCBI) database using the Basic Local Alignment Search Tool (BLAST). Additionally, we predicted the LhSorPR5 signal peptide at the N-terminus using Signal IP 4.1 (Petersen *et al*., 2011). We calculated the theoretical isoelectric point (pI) and molecular weight (MW) using the Compute pI/Mw tool. We conducted multiple alignment of protein sequences using the ClustalW program. Lastly, we constructed a PR5 protein phylogram applying the neighbor-joining method using Mega 4.1 software (Tamura *et al*., 2007).

Prediction of the Three-dimensional Structure of LhSorPR5 by Homology Modeling

We predicted the LhSorPR5 3D structure using the Swiss-Model (Biasini *et al*., 2014), a web-based protein structure prediction tool. Superposition of the built LhSorPR5 model on the corresponding template was conducted using the Swiss-PdbViewer. The root-mean-square deviation (RMSD), which measures the average distance between the backbone atoms of the superposed proteins, was calculated using PDBeFold (Velankar *et al*., 2010). We evaluated the stereochemical quality of the built LhSorPR5 model using PROCHECK V.3.5.4 (Laskowski *et al*., 1993). We then

generated the electrostatic potential of the built LhSorPR5 model and the template protein and mapped them to the surface of proteins using UCSF Chimera 1.11 (Pettersen *et al*., 2004).

Expression Analysis of *LhSorPR5* in Different Tissues and under Various Stress Treatments

We selected 30-days-old seedlings with similar growth performance to study LhSorPR5 expression profiling in response to different stress treatments. We conducted six stress treatments (sodium chloride (NaCl), polyethylene glycol (PEG), abscisic acid (ABA), methyl jasmonate (MeJA), ethephon (ETH), and sodium salicylate (SA)) and collected leaves 0, 2, 4, 8, 12 and 24 h after the initiation of the stress treatments. For the NaCl and PEG treatments, we drenched lily seedlings in 500 mL solutions containing 500 mM NaCl or 10% PEG. Seedlings drenched in equal volumes of ddH_2O served as the control for these two treatments. For the ABA and MeJA treatments, they were first dissolved in absolute ethanol and then diluted with ddH_2O to a final concentration of 2 µM and 20 mM, respectively, for foliar spraying. For these two treatments, we used water that contained the same ethanol concentration (1‰) as the control. For the ETH and SA treatments, on the other hand, we used solutions containing 5 mM ETH or 10 mM SA for foliar spraying of lily seedlings. Following this, we used a foliar application of pure water for the control treatment. For pathogen inoculation, *B. elliptica*, the causal agent of fire blight in lily was used. *B. elliptica* strain was first grown on potato dextrose agar (PDA) medium for 5 days. Conidia were collected by flooding the agar plates with 5 mL of Tween 20 solution (0.05% Tween 20 in sterile water) and scraped from the surface using a glass rod. After filtered by miracloth, concentration was adjusted to 8×10^5 conidia/mL using a hemocytometer for inoculation. Tween 20 solution was used as control for *B. elliptica* infection treatment. All samples collected were frozen immediately in liquid nitrogen and kept in a freezer at -80°C until use.

For *LhSorPR5* expression analysis in different tissues, we sampled roots, stems, leaves, petals, and scales from two months old fully bloomed lilies and subjected them to RNA isolation as described above. Furthermore, we reversely transcribed 500 ng of total RNA into cDNA using the HiScript II Q RT SuperMix for qPCR kit (Vazyme Biotech Co., Nanjing, China). After diluting with RNAse-free water, we used 20 ng of cDNA as the template for the subsequent qPCR step. We conducted qPCR using the AceQ qPCR SYBR Green Master Mix kit (Vazyme Biotech Co., Nanjing, China) following the manufacturer's instructions. We designed the primer set (LhSorPR5 qPCR-F and LhSorPR5 qPCR-R; Table 1) for the specific amplification of *LhSorPR5* using OligoArchitect, a platform for qPCR primer design developed by Sigma-Aldrich. We conducted all PCR reactions using the MX3000P qPCR thermo cycler (Stratagene, USA). The following protocol was used for amplification: pre-denaturation for 10 min at 95°C followed by 40 cycles at 94°C for 15 s and 60°C for 30 s. We used the lily *polyubiquitin 4* gene (GenBank accession no. DW718023) as a reference (Wang *et al*., 2017a) to calculate the relative expression. We calculated the relative expression using the relative expression software tool (REST 2009), and we used the P (H1) test for statistical analysis. Lastly, we used OriginPro 8.1 software to conduct all data plotting.

Prokaryotic Expression and Purification of LhSorPR5

To construct the pCold II-LhSorPR5 expression vector, we designated primers with EcoRI and SalI restriction sites (Table 1) to amplify the CDS of *LhSorPR5* (truncated form, devoid of signal peptide). The amplified PCR product was double digested and inserted into the pCold II vector. The recombinant pCold II-LhSorPR5 vector, verified by sequencing, was transformed in *Escherichia coli* Origami B (DE3) cells for protein expression. We inoculated a single colony of *E. coli* Origami B (DE3) cells containing LhSorPR5-pCold II vectors (designated LhSorPR5/OB) in 500 mL of liquid LB medium supplemented with 100 µg/mL ampicillin. This medium was shaken at 37°C until the optical density at 600 nm (OD600) reached from 0.4 to 0.5. After being incubated on ice for 30 min, we added isopropylthio-β-D-galactoside (IPTG) to the medium to a final concentration of 0.3 mM to induce protein expressions for another 48 h at 16°C. The culture was centrifuged at 5000 g for 10 min at 4°C to collect *E. coli* cells. After being twice washed in PBS, we resuspended the cell pellet in a lysis buffer (20 mM β-mercaptoethanol, 100 mM NaH_2PO4, 300 mM NaCl, 8 M urea; PH 8.0) and subjected it to cell lysis through sonication. We centrifuged the lysate at 12000 g for 10 min at 4°C, and we used the supernatant for LhSorPR5 purification using immobilized metal (Ni^{2+}) affinity chromatography (IMAC). Finally, we eluted the His-labeled LhSorPR5 recombinant protein with the lysis buffer supplemented with different concentrations of imidazole (20, 50, 100, 150, 200, 250, 300, 400 and 500 mM).

Western Blot Analysis

To detect the presence of His_6-labled proteins in *E. coli*, we conducted immunoblot analysis using a His_6 antibody. We initially subjected the cell lysate of LhSorPR5/OB and the pCold II empty vector control to sodium dodecyl sulfate polyacrylamide gel electrophoresis (SDS-PAGE; 18%). After electrophoresis, we transferred all proteins on the gel to the polyvinylidene difluoride (PVDF) membrane. Then added rabbit anti-His polyclonal antibody (Sangon Biotech, Shanghai, China) to bind specifically to His-labeled proteins. We used alkaline phosphatase conjugated goat anti-rabbit IgG (Sangon, Shanghai, China) as a secondary antibody, and we detected the existence of His-labeled proteins using the NTB/BCIP alkaline phosphatase kit (Sangon Biotech, Shanghai, China).

Table 1: List of primers used in the experiment

Experiment	Primer name	Primer sequence (5′–3′)
PR5 degenerate PCR	PR5-deg-F	CCNCCNGCNACNCTNGCNGARTT
	PR5-deg-R	TCRTCRTANGCRTARCTRTA
LhSorPR5 5′ RACE	LhSorPR5-5RACE-GSP-1	GGCTACCTTGCCACGCCATTTCACG
	LhSorPR5-5RACE-GSP-2	CCGTTCAGCTGCACTAAACACCCG
LhSorPR5 3′ RACE	LhSorPR5-3RACE-GSP-1	GCGGAGGCGGGAACAACTGCACTGC
	LhSorPR5-3RACE-GSP-2	TGCAAGCCGACCGTGTACTCAGAG
LhSorPR5 qPCR	LhSorPR5 qPCR-F	CGGCTGAACTGAAGGTAGTG
	LhSorPR5 qPCR -R	GGTAGAGGTGGCATCATCATAAG
Construction of the LhSorPR5 expression vector	LhSorPR5-OE-F	TAGACGAATTCTCTTTCTCGGCTACTTTTACCATCA
	LhSorPR5-OE-R	TAGACGTCGACAAATCGCCGCTGCAAAAGCAA

Restriction sites for vector construction are underlined

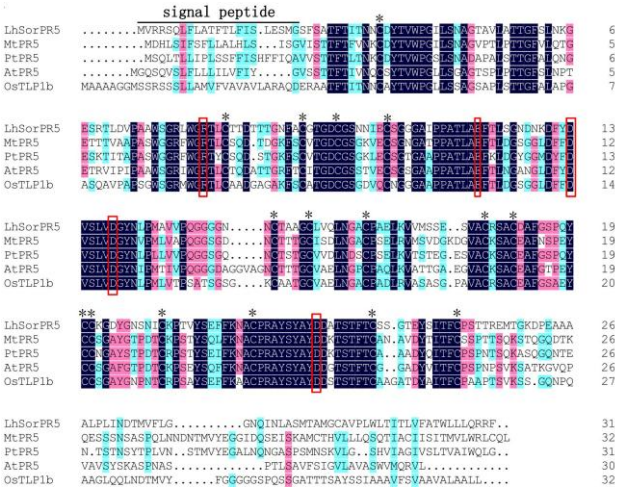

Fig. 1: Sequence alignment of LhSorPR5, including PR5s from other plants. Alignment of the putative amino acid sequence of LhSorPR5 with sequences from *Medicago truncatula* (MtPR5) (GenBank accession no. XP_003589504), *Populus trichocarpa* (PtPR5) (GenBank accession no. XP_002306938), *Arabidopsis thaliana* (AtPR5) (GenBank accession no. AEE86602), and *Oryza sativa* (OsTLP1b) (GenBank accession no. XP_015612927). Identical residues are shaded in dark blue, highly similar residues are shaded in pink, and similar residues are shaded in light blue. Predicted signal peptides are highlighted by an upper line. The red boxes represent the REDDD motifs that form the acidic cleft. The 16 cysteines responsible for the formation of the disulfide bridges are indicated by an asterisk (*)

Results

Molecular Cloning and Sequence Analysis of LhSorPR5

We obtained a 353 bp long fragment from the degenerate PCR, and the homology of the partial coding sequence that we obtained was confirmed by BLAST. After obtaining the 5′RACE and 3′RACE PCRs, we assembled the *LhSorPR5* full-length sequence. The *LhSorPR5* cDNA we obtained was 1391 bp in length, comprising of a 5′ untranslated region (UTR) of 137 bp, a predicted ORF of 939 bp, and a 3′ UTR of 315 bp. The *LhSorPR5* gene encoded a protein of 312 amino acids with a predicted 22 amino acid signal peptide (Fig. 1) located at the N-terminus. The calculated theoretical pI and molecular weight were 4.5 and 30.49 kDa, respectively. We submitted the LhSorPR5 cDNA sequence to GenBank, which was deposited under the accession number KY273923.

Multiple sequence alignment revealed that LhSorPR5 shared high levels of identity and similarity with PR5s originating from other plants. For instance, LhSorPR5 shared 59.41% similarity with ZmTLP1, 63.39% with TcPR5, and 58.88% with OsTLP1b. As a member of the PR5 family of proteins, LhSorPR5 shared several domains with other orthologs. In total, 16 cysteine residues (Fig. 1), forming eight pairs of disulfide bridges, were conserved in LhSorPR5. The five amino acids and REDDD, which form the acidic cleft, were also highly conserved across species.

We constructed a phylogram to explore phylogenetic relationships between LhSorPR5 and other PR5s. As shown in Fig. 2, LhSorPR5 was closely correlated to ZmTLP1, TcPR5, and OsTLP1b. These results demonstrated that LhSorPR5 is a member of the PR5 family of proteins and could therefore be involved in lily defense-related processes.

Prediction of the Three-dimensional Structure of LhSorPR5 by Homology Modeling

We submitted the LhSorPR5 protein sequence to the SWISS-MODEL server to automatically conduct protein structure modeling. The 3D structure of Pru av 2 (2ahn.1.A), a thaumatin-like protein originating from *Prunus avium* cv. Germersdorfer, was used as the template to build the LhSorPR5 3D model. The 3D structures of LhSorPR5 and the Pru av 2 are shown in Fig. 3A and Fig. 3B, respectively. Superposition of the LhSorPR5 3D model with the Pru av 2 template revealed that the 3D structures of these two proteins were highly similar (Fig. 3C). The RMSD value calculated for the superposed proteins was 0.44, which indicated a high similarity in 3D structure between these two proteins. Our stereochemical quality check of the built LhSorPR5 model showed that 88.2% and 11.8% of residues were either in the most favorable regions or the additional regions allowed, respectively.

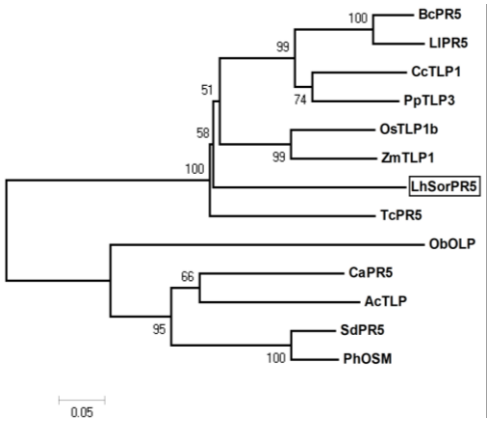

Fig. 2: Phylogram of LhSorPR5 with PR5 proteins from other plant species. Phylogenetic relationships between LhSorPR5 and *Brassica campestris* (BcPR5) (GenBank accession no. A8IXG8), *Lepidium latifolium* (LlPR5) (GenBank accession no. D0ELG2), *Cajanus cajan* (CcTLP1) (GenBank accession no. KYP38775), *Prunus persica* (PpTLP3) (GenBank accession no. G9CM55), *Oryza sativa* (OsTLP1b) (GenBank accession no. XP_015612927), *Zea mays* (TLP1) (GenBank accession no. ACG39784), *Theobroma cacao* (PR5) (GenBank accession no. XP_007046683), *Ocimum basilicum* (ObOLP) (GenBank accession no. AGX15390), *Curcuma amada* (PR5) (GenBank accession no. AEH41422), *Actinidia chinensis* (AcTLP) (Genbank accession no. AGC39176), *Solanum dulcamara* (PR5) (GenBank accession no. AAG16625), and *Petunia* × *hybrida* (PhOSM) (GenBank accession no. AAK55411). Branch length is proportional to the time of divergence. The scale bar represents a change of 5%. LhSorPR5 is highlighted by a solid line box

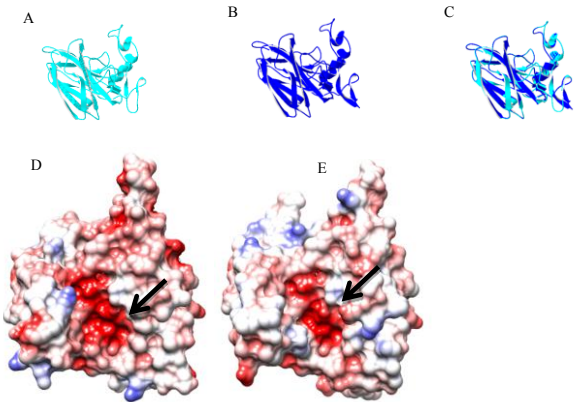

Fig. 3: The predicted three-dimensional structure of LhSorPR5 with Pru-TLP (2ahn.1.A) we used as the template. (A) Predicted structure of LhSorPR5. (B) Structure of the Pru-TLP used as the template for modeling. (C) Superposition of the predicted LhSorPR5 model with the Pru-TLP template. (D) Surface topology of the predicted LhSorPR5 model showing the electrostatic potential. (E) Surface topology of the Pru-TLP template showing the electrostatic potential. The conserved acidic cleft, which catalyzes hydrolysis of β-1,3-glucan, is indicated by an arrow

Previous studies have shown that acidic clefts are a common feature in antifungal PR5 family proteins (Koiwa *et al*., 1999; Ghosh and Chakrabarti, 2008). To reveal the presence of the acidic cleft, we calculated the eletrostatic potential of the built LhSorPR5 model (Fig. 3D) and the Pru av 2 template (Fig. 3E). The acidic cleft can be detected at the surface of these two proteins (see Fig. 3). The presence of the acidic cleft, which is the binding site for β-glucan, showed that LhSorPR5 could function in a similar manner to the glucanase activity exhibited by other members of the PR5 family.

Tissue-specific Expressions of *LhSorPR5*

For *LhSorPR5* expression analysis by qPCR, we first plotted standard curves and dissociation curves to determine amplification efficiency and to test amplification specificity. We quantified the relative expression levels of *LhSorPR5* in different tissues using expression levels in stems as a calibrator (set at 1.0). As shown in Fig. 4, we observed the highest *LhSorPR5* expression in stems. *LhSorPR5* expression levels in scales were significantly lower than in stems (by a factor of 0.35). Expression levels in petals, roots, and leaves were all lower than in stems, although not statistically significant.

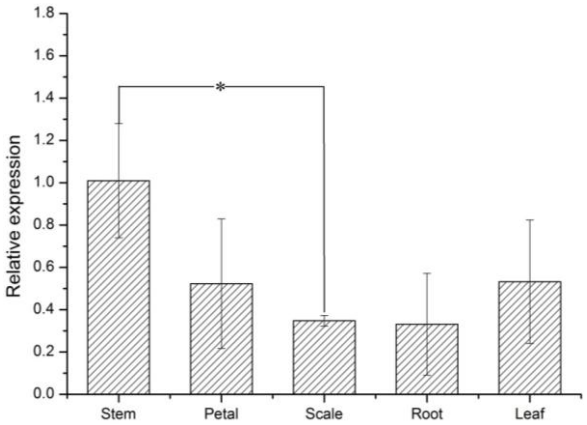

Fig. 4: Tissue-specific expression of *LhSorPR5*. We used the *LhSorPR5* transcript level in stems as a calibrator (set at 1.0) to determine the relative expression in different tissues. We used REST (2009) software to calculate the relative expression, and values for the three replicates are shown as means ± standard deviations (SD). Bars labeled with an asterisk (*) indicate significant differences from the calibrator (stem) at $P<0.05$ (the REST statistical randomization test)

LhSorPR5 Expression Analysis in Response to Various Stress Treatments

To investigate whether *LhSorPR5* expressions were induced

by stress, we quantified *LhSorPR5* transcript levels after conducting MeJA, SA, ETH, ABA, NaCl and PEG treatments. Following the MeJA treatment, the temporal *LhSorPR5* expression exhibited an accumulating pattern over time (Fig. 5A), reaching its highest level 24 h after treatment (by a factor of 6.06 compared to the control). Foliar spraying of SA also significantly induced *LhSorPR5* expressions 4 h after treatment by a factor of 3.31 compared to the control (Fig. 5B). For the ETH treatment (Fig. 5C), *LhSorPR5* expressions were rapidly upregulated 2 h after treatment (by a factor of 4.18 compared to the control). When subjected to the ABA treatment (Fig. 5D), *LhSorPR5* transcriptions were significantly induced 4 h after treatment, reaching its peak level 8 h after treatment. Furthermore, NaCl stress (Fig. 5E) significantly induced *LhSorPR5* expressions at all time points after the treatment was initiated. We observed the highest expression 4 h after NaCl stress was imposed. Moreover, we found that PEG (Fig. 5F) induced osmotic stress also stimulated the *LhSorPR5* expression and *LhSorPR5* transcript levels were significantly different from the control 2 h, 12 h and 24 h after the PEG treatment. Besides, inoculation of *B. elliptica* (Fig. 5G), the causal agent of fire blight in lily, also significantly induced *LhSorPR5* expression 4 h, 12 h, 24 h and 48 h after pathogen infection. The upregulation of *LhSorPR5* that we observed in response to biotic and abiotic stress suggested that *LhSorPR5* could be widely involved in the defense response of different types of lilies.

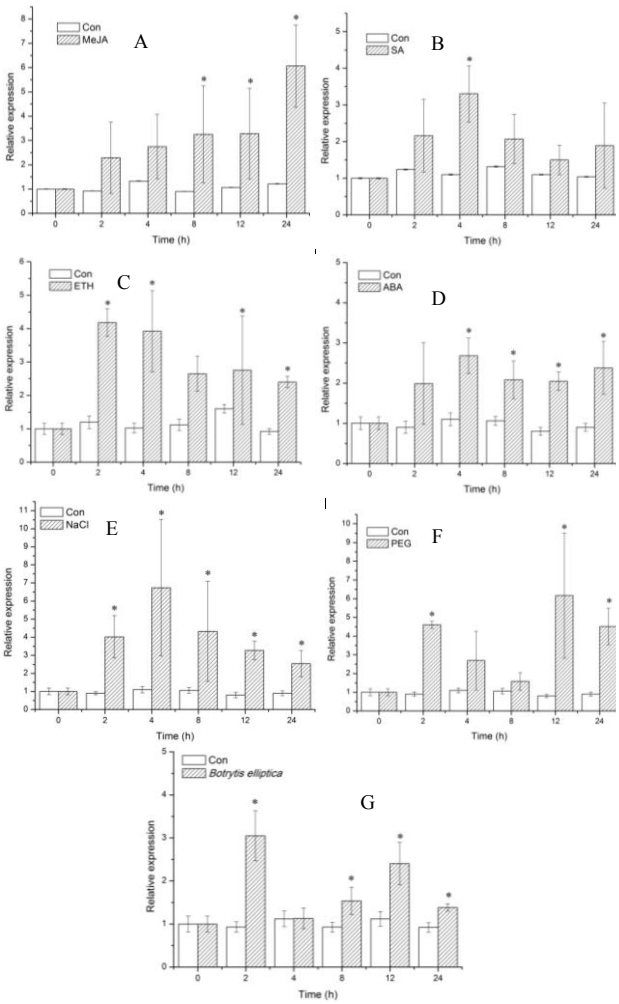

Fig. 5: *LhSorPR5* expressions in response to various stress treatments. (A) *LhSorPR5* expression in response to the methyl jasmonate (MeJA) treatment. (B) *LhSorPR5* expression in response to the sodium salicylate (SA) treatment. (C) *LhSorPR5* expression in response to the ethephon (ETH) treatment. (D) LhSorPR5 expression in response to the abscisic acid (ABA) treatment. (E) *LhSorPR5* expression in response to the NaCl treatment. (F) *LhSorPR5* expression in response to the PEG treatment. (G) *LhSorPR5* expression in response to *Botrytis elliptica* infection. We used the *LhSorPR5* expression at 0 h as a calibrator (designated 1.0) to determine the relative expression of the target gene at different time points. Values are shown as means ± standard deviations (SD) for the three replicates. Bars labeled with an asterisk (*) indicate significant differences from the control at $P<0.05$ (the REST statistical randomization test)

Heterologous Expressions of LhSorPR5 in *E. coli*

We inserted the CDS of *LhSorPR5* (devoid of signal peptide) into the pCold II vector, and we were able to successfully expressed the His_6-tagged LhsSorPR5 recombinant in *E. coli* cells. As shown in Fig. 6A, we detected the presence of the LhSorPR5 recombinant protein (~33kDa) in the insoluble fraction of LhSorPR5/OB cells (Fig. 6A; Lane 4), while we observed no visible band of corresponding size in the pCold II/OB control. To further confirm the presence of the LhSorPR5 recombinant protein, we conducted immunoblot analysis with the anti-His_6 antibody, and we specifically detected His_6-tagged LhSorPR5 (Fig. 6B; Lane 4). We subjected the recombinant LhSorPR5 to purification (Fig. 6C) with the Ni-NTA column, and the optimized condition for recombinant LhSorPR5 purification was at a concentration of 300 mM imidazole (Fig. 6C; Lane 7). Although attempts to renature the purified LhSorPR5 were unsuccessful, the recombinant LhSorPR5 purified in our study could be used in the production of antibodies in future studies.

Discussion

In this study, we isolated a novel thaumatin-like protein from the oriental hybrid lily Sorbonne cultivar (designated LhSorPR5). Sequence alignment of the LhSorPR5 protein to other PR5s revealed that the 16 cysteine residues, which were responsible for the formation of eight pairs of disulfide bridges, were highly conserved in LhSorPR5. After we built the LhSorPR5 3D model, we found the acidic cleft, which is the docking site for β-glucans, in LhSorPR5. β-1,3-glucan is one of the key component found in fungal cell walls. The

acidic cleft catalyzed β-glucan hydrolysis, and glucanase activity was found to be an important contributor to antifungal activity of PR5 family proteins as suggested by other studies (Grenier *et al*., 1999; Ghosh and Chakrabarti, 2008). However, mechanisms by which PR5s exert antifungal activity remain elusive owing to the fact that some TLPs (Mal-TLP and Pru-TLP), which possess moderate endo β-1,3-glucanase activity, exhibited no antifungal activity (Menu-Bouaouiche *et al*., 2003). It has been reported that PR5 proteins inhibit spore germination and hyphal growth by increasing the permeability of fugal membranes (Abad *et al*., 1996; Chowdhury *et al.,* 2015). Hence, membrane leakage caused by pore formation during interactions between PR5 proteins and fungal membranes has been proposed as another possible mechanism for the antifungal activity exhibited in PR5 family proteins (Roberts and Selitrennikoff, 1990).

As important participants in plant defense mechanisms, we observed the induction of PR proteins not only during biotic stress but also under adverse conditions of abiotic stress. For *Arabidopsis*, *PR1*, *PR2* and *PR5* expressions were induced by the biotrophic fungus pathogen *Peronospora parasitica* (Penninckx *et al*., 1996) as well as drought stress (Liu *et al*., 2013). For monocot rice plant species, expressions of two *PR5* genes were induced by means of *Rhizoctonia solani* infection (Velazhahan *et al*., 1998), and transcript levels of *PR4* paralogues were differentially regulated by various stress types (Wang *et al*., 2011b). Moreover, *O. basilicum* (Misra *et al*., 2016) and peanut (Singh *et al*., 2013) *PR5* expressions were significantly induced by pathogen inoculation, salt stress, and dehydration. In our study, *LhSorPR5* expressions were significantly induced by the exogenous application of phytohormones (SA, MeJA, ETH and ABA) as well as salt and PEG stress, implying that *LhSorPR5* is widely involved in the defense signaling pathways mediated by these hormones. Growing evidence reveals that SA, JA and ET are major hormones that regulate plant immunity (Pieterse *et al*., 2009), and SA, JA and ET mediated signaling pathways are crucial to plant defense against fungal, bacterial, and viral pathogens. Induction of *LhSorPR5* by SA, JA, and ET indicated that the *LhSorPR5* cloned in this study could be involved in lily disease resistance. Given that *PR5* is considered a marker gene for SA signaling pathways, the characterization of *LhSorPR5* in this study could potentially make it a marker gene candidate for SA response in lilies.

Conclusion

This study characterized LhSorPR5, the first PR5 orthologue cloned from lilies. Homology modeling revealed that an acidic cleft is a feature of LhSorPR5, which may enable β-glucan binding and enable the protein to conduct glucanase activity. Our expression analysis results showed that *LhSorPR5* was significantly induced by salinity, drought stress, pathogen infection and the presence of phytohormones (such as MeJA, SA, ETH and ABA). To conclude, the production of lily bulbs and cut flowers are severely affected by both pathogens and environmental stress, such as salt concentrations and drought stress. The characterization of PR proteins, including LhSorPR5, could increase our understanding of lily immunity and facilitate the genetic engineering of lilies in the future.

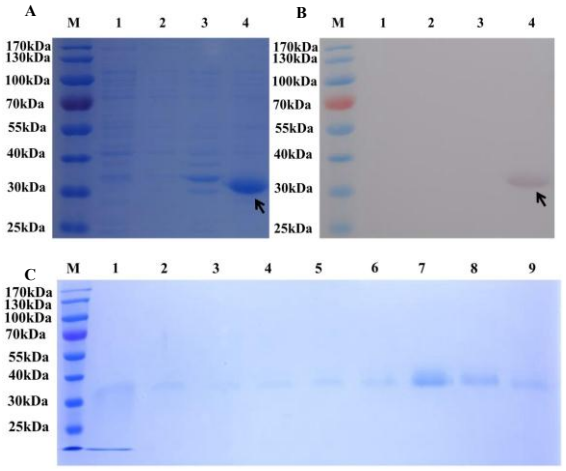

Fig. 6: Expression of His_6-tagged LhSorPR5 in *Escherichia coli* Origami B cells, western blot analysis, and purification. (A) SDS-PAGE analysis of LhSorPR5 recombinant proteins. Lane M, protein marker; Lane 1, soluble protein fraction of *Escherichia coli* cells harboring pCold II vectors with IPTG induction; Lane 2, insoluble protein fraction of *Escherichia coli* cells harboring pCold II vectors with IPTG induction; Lane 3, soluble protein fraction of *Escherichia coli* cells harboring LhSorPR5-pCold II vectors with IPTG induction; Lane 4, insoluble protein fraction of *Escherichia coli* cells harboring LhSorPR5-pCold II vectors with IPTG induction. The recombinant LhSorPR5 protein expressed in the insoluble fraction is indicated by an arrow. (B) Detection of His-labeled LhSorPR5 with an His_6-polyclonal antibody. Loading of protein samples followed the same procedure as shown in Fig. 6A. The His_6-tagged recombinant LhSorPR5 detected is indicated by an arrow. (C) Purification of His-labeled LhSorPR5 with IMAC. The recombinant protein loaded on the Ni-NTA column was eluted with buffers containing increasing concentrations of imidazole. Lane M, protein marker; Lane 1–9, SDS-PAGE analysis of eluate that flowed through the Ni-NTA column. The loaded LhSorPR5 recombinant protein was washed by an elution buffer containing 20, 50, 100, 150, 200, 250, 300, 400, and 500 mM imidazole (Lane 1–9)

Acknowledgements

This research was supported by the Ningxia Agricultural Comprehensive Development Office (NTKJ2015-05-01), the National Natural Science Foundation of China (No. 31101190 and No. 31201651), the CAS Key Technology Talent Program (No. 2016-65), the "West Light" project of

the Chinese Academy of Sciences in 2014, the China Postdoctoral Science Foundation funded project (No. 2015M580894), and the Hundred Talents Programs of Chinese Academy of Sciences (No. Y629721002 and No. 27Y127L41002).

References

Abad, L.R., M.P. DUrzo, D. Liu, M.L. Narasimhan, M. Reuveni, J.K. Zhu, X.M. Niu, N.K. Singh, P.M. Hasegawa and R.A. Bressan, 1996. Antifungal activity of tobacco osmotin has specificity and involves plasma membrane permeabilization. *Plant Sci*., 118: 11–23

Anzlovar, S. and M. Dermastia, 2003. The comparative analysis of osmotins and osmotin-like PR-5 proteins. *Plant Biol*., 5: 116–124

Biasini, M., S. Bienert, A. Waterhouse, K. Arnold, G. Studer, T. Schmidt, F. Kiefer, T.G. Cassarino, M. Bertoni, L. Bordoli and T. Schwede, 2014. SWISS-MODEL: modelling protein tertiary and quaternary structure using evolutionary information. *Nucleic Acids Res*., 42: W252–W258

Buschman, J.C.M., 2005. Globalisation-flower - flower bulbs - bulb flowers. *Acta Hort.*, 673: 27-33

Chowdhury, S., A. Basu and S. Kundu, 2015. Cloning, characterization, and bacterial over-expression of an ssmotin-like protein gene from *Solanum nigrum* L. with antifungal activity against three necrotrophic fungi. *Mol. Biotechnol*., 57: 371–381

Cornelissen, B.J.C., R.A.M.H. Vanhuijsduijnen and J.F. Bol, 1986. A tobacco mosaic virus-induced tobacco protein is homologous to the sweet-tasting protein thaumatin. *Nature,* 321: 531–532

Curir, P., L. Guglieri, M. Dolci, A. Capponi and G. Aurino, 2000. Fusaric acid production by *Fusarium oxysporum* f.sp lilii and its role in the lily basal rot disease. *Eur. J. Plant Pathol*., 106: 849–856

Edens, L., L. Heslinga, R. Klok, A.M. Ledeboer, J. Maat, M.Y. Toonen, C. Visser and C.T. Verrips, 1982. Cloning of cDNA encoding the sweet-tasting plant protein thaumatin and its expression in *Escherichia coli*. *Gene*, 18: 1–12

Ghosh, R. and C. Chakrabarti, 2008. Crystal structure analysis of NP24-I: a thaumatin-like protein. *Planta*, 228: 883–890

Glazebrook, J., 2005. Contrasting mechanisms of defense against biotrophic and necrotrophic pathogens. *Annu. Rev. Phytopathol*., 43: 205–227

Grenier, J., C. Potvin, J. Trudel and A. Asselin, 1999. Some thaumatin-like proteins hydrolyse polymeric beta-1,3-glucans. *Plant J*., 19: 473–480

Jones, J.D. and J.L. Dangl, 2006. The plant immune system. *Nature*, 444: 323–329

Koiwa, H., H. Kato, T. Nakatsu, J. Oda, Y. Yamada and F. Sato, 1999. Crystal structure of tobacco PR-5d protein at 1.8 angstrom resolution reveals a conserved acidic cleft structure in antifungal thaumatin-like proteins. *J. Mol. Biol*., 286: 1137–1145

Laskowski, R.A., M.W. Macarthur, D.S. Moss and J.M. Thornton, 1993. Procheck-a program to check the stereochemical quality of protein structures. *J. Appl. Crystallogr*., 26: 283–291

Liu, W.X., F.C. Zhang, W.Z. Zhang, L.F. Song, W.H. Wu and Y.F. Chen, 2013. *Arabidopsis* Di19 functions as a transcription factor and modulates *PR1*, *PR2*, and *PR5* expression in response to drought stress. *Mol. Plant*, 6: 1487–1502

Liu, Y.H., C.J. Huang and C.Y. Chen, 2008. Evidence of induced systemic resistance against *Botrytis elliptica* in lily. *Phytopathology*, 98: 830–836

Menu-Bouaouiche, L., C. Vriet, W.J. Peumans, A. Barre, E.J.M. Van Damme and P. Rouge, 2003. A molecular basis for the endo-beta 1,3-glucanase activity of the thaumatin-like proteins from edible fruits. *Biochimie*, 85: 123–131

Misra, R.C., Sandeep, M. Kamthan, S. Kumar and S. Ghosh, 2016. A thaumatin-like protein of *Ocimum basilicum* confers tolerance to fungal pathogen and abiotic stress in transgenic *Arabidopsis*. *Sci. Rep.,* 6: 25340

Niimi, Y., D.S. Han, S. Mori and H. Kobayashi, 2003. Detection of cucumber mosaic virus, lily symptomless virus and lily mottle virus in Lilium species by RT-PCR technique. *Sci. Hort*., 97: 57–63

Penninckx, I.A.M.A., K. Eggermont, F.R.G. Terras, B.P.H.J. Thomma, G.W. DeSamblanx, A. Buchala, J.P. Metraux, J.M. Manners and W.F. Broekaert, 1996. Pathogen-induced systemic activation of a plant defensin gene in Arabidopsis follows a salicylic acid-independent pathway. *Plant Cell*, 8: 2309–2323

Petersen, T.N., S. Brunak, G. von Heijne and H. Nielsen, 2011. SignalP 4.0: discriminating signal peptides from transmembrane regions. *Nat. Meth.*, 8: 785–786

Pettersen, E.F., T.D. Goddard, C.C. Huang, G.S. Couch, D.M. Greenblatt, E.C. Meng and T.E. Ferrin, 2004. UCSF Chimera-A visualization system for exploratory research and analysis. *J. Comput. Chem*., 25: 1605–1612

Pieterse, C.M.J., A. Leon-Reyes, S. Van der Ent and S.C.M. Van Wees, 2009. Networking by small-molecule hormones in plant immunity. *Nat. Chem. Biol*., 5: 308–316

Roberts, W.K. and C.P. Selitrennikoff, 1990. Zeamatin, an antifungal protein from maize with membrane permeabilizing activity. *J. Gen. Microbiol*., 136: 1771–1778

Rout, E., S. Nanda and R.K. Joshi, 2016. Molecular characterization and heterologous expression of a pathogen induced PR5 gene from garlic (*Allium sativum* L.) conferring enhanced resistance to necrotrophic fungi. *Eur. J. Plant Pathol*., 144: 345–360

Singh, N.K., K.R.R. Kumar, D. Kumar, P. Shukla and P.B. Kirti, 2013. Characterization of a pathogen induced thaumatin-like protein gene *AdTLP* from *Arachis diogoi*, a wild peanut. *PLoS ONE*, 8: e83963

Singh, N.K., C.A. Bracker, P.M. Hasegawa, A.K. Handa, S. Buckel, M.A. Hermodson, E. Pfankoch, F.E. Regnier and R.A. Bressan, 1987. Characterization of osmotin: a thaumatin-like protein associated with osmotic adaptation in plant cells. *Plant Physiol*., 85: 529–536

Tamura, K., J. Dudley, M. Nei and S. Kumar, 2007. MEGA4: molecular evolutionary genetics analysis (MEGA) software version 4.0. *Mol. Biol. Evol*., 24: 1596–1599

van Loon, L.C., M. Rep and C.M.J. Pieterse, 2006. Significance of inducible defense-related proteins in infected plants. *Annu. Rev. Phytopathol*., 44: 135–162

Velankar, S., C. Best, B. Beuth, C.H. Boutselakis, N. Cobley, A.W.S. Da Silva, D. Dimitropoulos, A. Golovin, M. Hirshberg, M. John, E.B. Krissinel, R. Newman, T. Oldfield, A. Pajon, C.J. Penkett, J. Pineda-Castillo, G. Sahni, S. Sen, R. Slowley, A. Suarez-Uruena, J. Swaminathan, G. van Ginkel, W.F. Vranken, K. Henrick and G.J. Kleywegt, 2010. PDBe: Protein data bank in Europe. *Nucleic Acids Res*., 38: D308–D317

Velazhahan, R., K. Chen-Cole, C.S. Anuratha and S. Muthukrishnan, 1998. Induction of thaumatin-like proteins (TLPs) in *Rhizoctonia solani*-infected rice and characterization of two new cDNA clones. *Physiol. Plantarum*, 102: 21–28

Wang, L., Z.H. Guo, Y.B. Zhang, Y.J. Wang, Y. Guo, Y. Liu, R.Y. Wang and Z.K. Xie, 2017a. Characterization of *LhSorP5CS*, a gene catalyzing proline synthesis in Oriental hybrid lily Sorbonne: molecular modelling and expression analysis. *Bot. Stud*., 58: 10

Wang, N.L., B.Z. Xiao and L.Z. Xiong, 2011b. Identification of a cluster of PR4-like genes involved in stress responses in rice. *J. Plant Physiol*., 168: 2212–2224

Zhang, Y.B., Y.J. Wang, W.R. Yang, Z.K. Xie, R.Y. Wang, H.R. Kutcher and Z.H. Guo, 2015a. A rapid immunochromatographic test to detect the lily mottle virus. *J. Virol. Methods*, 220: 43–48

Zhang, Y.B., Y.J. Wang, J. Meng, Z.K. Xie, R.Y. Wang, H.R. Kutcher and Z.H. Guo, 2015b. Development of an immunochromatographic strip test for rapid detection of lily symptomless virus. *J. Virol. Meth*., 220: 13–17

(Received 06 December 2016; Accepted 25 April 2017)